Numerical modelling of thermal comfort in non-uniform environments using real-time coupled simulation models

Babich F, Cook MJ, Loveday DL, Cropper PT. **Numerical modelling of thermal comfort in non-uniform environments using real-time coupled simulation models.** *In: Proceedings of Building Simulation and Optimisation 2016: 3rd IBPSA-England Conference.* Newcastle upon Tyne; 2016. p 4-11

NUMERICAL MODELLING OF THERMAL COMFORT IN NON-UNIFORM ENVIRONMENTS USING REAL-TIME COUPLED SIMULATION MODELS

Francesco Babich[1], Malcolm Cook[1], Dennis Loveday[1], and Paul Cropper[2]
[1]Loughborough University, School of Civil and Building Engineering, LE11 3TU Loughborough, UK
[2]Institute of Energy and Sustainable Development, De Montfort University, LE1 9BH Leicester, UK

ABSTRACT

This research aimed to test and validate the only existing real-time coupled model of human thermal comfort by comparing simulation results and measured data for a number of different realistic non-uniform scenarios. This model incorporates detailed and realistic human figures in CFD, coupled with the IESD-Fiala model which enables the reaction of human occupants and their influence on the environment by heat and mass transfer to be modelled. A set of likely configurations have been created in an environmental chamber. Typical furniture, a thermal manikin and a portable fan have been used to generate non-uniform controlled environments, and detailed measurements have been taken. The same configurations have been modelled using the coupled model. The initial results highlight that this coupled model can effectively predict human thermal comfort in non-uniform environments, being able to represent dynamic conditions around the body in real time. Further work is addressing more complex configurations.

INTRODUCTION

Buildings contribute more greenhouse gas emissions than either the industrial or the transportation sectors, primarily due to space cooling and heating energy use, driven by the basic human need for thermal comfort and good indoor air quality.

Traditional thermal comfort models such as the predicted mean vote – percentage of people dissatisfied (PMV-PPD) model (Fanger, 1970) and the more recent adaptive approach (de Dear and Brager, 1998) have limited use for complex transient and asymmetrical conditions. However, focusing on non-uniform thermal environments is important because the space conditioning systems that generate them are often likely to be less energy consuming than those which provide more homogeneous conditions.

Research conducted at University of California Berkeley (UCB) extensively analysed the effect of air movement on thermal comfort. Recent studies found that with personalised air movement, thermal comfort can be maintained up to 30 C and 60% relative humidity (RH), and perceived indoor air quality (IAQ) up to 80% RH (Zhai et al, 2015). Although participants' age and ethnic group may affect the results, many other similar studies support the idea that air movement improves thermal sensation in warm and hot conditions.

In order to improve the capability of the PMV/PPD method while dealing with non-uniform air movement conditions, indexes such as the standard equivalent temperature (SET*) derived from Gagge 2-Node model (Gagge et at, 1971) have been integrated in the PMV calculation in ASHRAE 55 (ASHRAE, 2013). However, this method still has several limitations: there is a single value of the air speed for the entire body, the air direction is not considered, and the spatial variation of any other boundary condition is not taken into account. Moreover, the model does not predict how the thermal sensation varies experiencing a given environment for a certain amount of time. It simply assumes that steady state conditions have been reached.

When environments that are more complex are studied, a more detailed model may provide with better results. The IESD-Fiala model (Fiala et al, 1999; Fiala et al, 2001) and the UCB model (Huizenga et al, 2001), both based on a multi-node model developed for aerospace applications (Stolwijk, 1970), are the two most advanced and currently used models.

The IESD-Fiala model is made by two complementary systems, namely the active (Fiala et al, 2001) and passive (Fiala et al, 1999) system. The former simulates the physiological phenomena by considering self-regulatory responses, which are vasoconstriction, vasodilatation, shivering and sweating. The latter estimates the heat exchange process inside the body, and between the body and its surroundings. In this model, the human body is subdivided into 19 spherical and cylindrical elements and there are 59 areas of the body surface.

The IESD-Fiala model has been extensively validated and is able to accurately predict the thermal sensation in dynamic conditions (Foda et al, 2011), and it has been successfully and entirely coupled with a CFD commercial code (Cropper et al, 2010). Entirely means fully automated, and the exchange of information between the two components of the model continues until both reach a converged

solution for each time step. As a result, the human dynamic thermal sensation (DTS) can be accurately predicted for a given non-uniform environment.

This coupled system was initially used to model a person in a naturally ventilated environment (Cropper et al, 2010), and to simulate buoyancy-driven natural ventilation in a school classroom (Cook et al, 2011), but there is still no complete validation of the coupled model using measured data from either real buildings or thermal chambers.

Therefore, the research presented in this paper aims to test and validate the coupled model by comparing simulation results and measured data for a number of different realistic scenarios.

METHODS

To achieve the aim of the study, two likely configurations have been created in an environmental chamber. Typical furniture, a thermal manikin and devices such as portable fans have been used to generate non-uniform controlled environments, and detailed measurements have been taken. These include air temperature (T_{air}), mean radiant temperature (MRT), RH and air speed (S_{air}) at several points within the room. The same configurations have then been modelled using the coupled CFD and IESD-Fiala model, and simulations have been run. Actual values and computer-based predictions have been compared, and the reasons for differences analysed.

Experimental set-up

Environmental chambers have been used in thermal comfort studies since the early stages of research in this field, and both human participants and thermal manikins have been used. The latter were especially used to provide accurate data for the validation of CFD models (Gao and Niu, 2005), highlighting the importance of an accurate representation of the human body shape when studying the micro-environment around a person, and that the radiative heat transfer cannot often be overlooked.

For this research, a rectangular environmental chamber located at Loughborough University has been used, together with a thermal manikin 'Victoria' seated in the room (manikin 'breathing' capability turned off), as shown in Figure 1. Use of a manikin provides an objective and repeatable human-shaped heat source for comparative testing. Moreover, a common desk-fan has been placed on the floor inside the chamber to provide air movement.

During the entire experiment, Victoria was wearing panties, a shirt, a thick sweater, trousers, socks and shoes. The manikin is divided into 16 body parts, and they were all kept at a constant surface temperature, 34°C. This is done by the software that controls Victoria, which increases or reduces the amount of power that is supplied to each body part. The power required to maintain a constant temperature provides a measure of the rate of heat loss to the surrounding environment. Thus, the higher the insulation provided by the clothing, the lower the power required to maintain the 34°C temperature.

Figure 1 The experimental facilities

Air was supplied to the chamber via a low-level inlet, and could leave the space only through a roof-level opening, which can be identified in Figure 2. The door was closed while taking any set of measurements, and the windows cannot be opened. Moreover, due to their multi-glazed well insulating structure, the internal surface temperature of the windows can be assumed equal to the temperature of the surrounding wall. Indeed these windows only provide a visual connection to the outside.

The environmental chamber has been warmed up using the walls, inside which there are pipes in which hot water circulates, and pre-heating the air entering into the room. Having left the room warming up for 24 hours, due to the severe outdoor winter conditions, the maximum T_{air} achievable was between 25°C and 26°C.

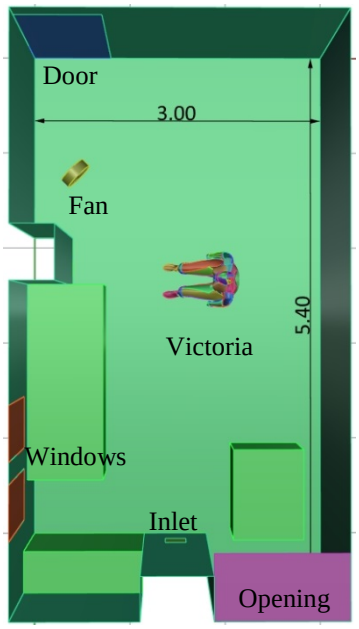

Figure 2 Chamber floor plan (dimensions in m)

Measurements have been taken with U12 Hobo sensors (Onset, 2015) and with Dantec ComfortSense kit (Dynamics Dantec, 2015), whose characteristics are summarised in Table 1. One U12 sensor has been placed in the inlet and one in the opening to measure the RH and the temperature of the air going into and out of the chamber. A complete Dantec kit has been placed close to Victoria, measuring T_{air} and S_{air} at three heights (from the floor: 0.1 m, 0.6 m, and 1.1 m), operative temperature (T_O) and RH (see Figure 1). Other two probes have been placed respectively 50 cm above the head of the manikin and in front of the inlet. The former has been used to gain information about the thermal plume, the latter to measure the S_{air} at the inlet.

Table 1

Measurement equipment characteristics

FEATURE	HOBO U12	DANTEC
Measurement range	T_{air}: -20 to 70 °C RH: 5 to 95 %	T_{air}: -20 to 80 °C RH: 0 to 100 % T_o: 0 to 45 °C S_{air}: 0.1 to 30 m/s
Accuracy	T_{air}: ± 0.35 °C RH: ± 2.5 %	T_{air}: ± 0.5 °C RH: ± 1.5% T_o: ±0.2 °C S_{air}: ± 2 % of reading (OR) ± 0.02 m/s
Response time	T_{air}: 6 minutes RH: 1 minute	T_{air}: 4-5 s RH: 10 minutes T_o: 2 minutes S_{air}: 2-3 s

Two sets of measurements have been taken. In both cases the measurement equipment was identical, and data have been recorded for 50 minutes. However, during the first test, the fan was switched off, while during the second it was operating. Therefore, the effect of higher S_{air} on the predicted thermal sensation can be assessed.

Modelling approach and assumptions

A model of the environmental chamber as it was during the measurements has then been built. Since the coupled model uses ANSYS CFX 14.5.7 (ANSYS, 2015), the first steps have been generating a geometry and then a mesh that could be imported into this program.

Firstly, due to the complexity of the human shape, an STL (STereoLithography) file has been simplified using MeshLab (MeshLab, 2016), and then imported into Rhinoceros (Rhino, 2016), in which NURBS (non-uniform rational basis spline) have been generated. The virtual manikin is then divided into parts, whose names must match those used by the IESD-Fiala model. In general, the remaining part of the geometry could be built either in Rhinoceros or in ICEM CFD.

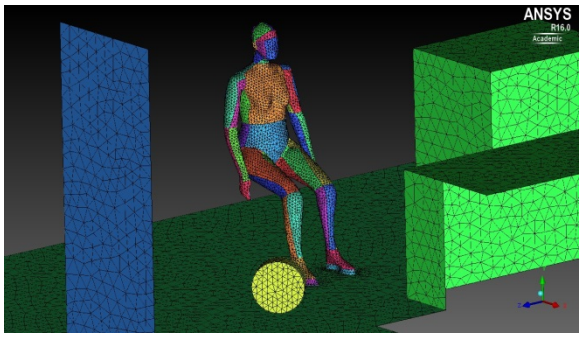

Figure 3 Shell mesh

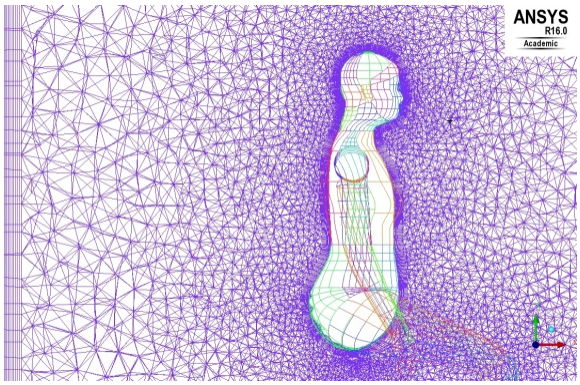

Figure 4 Volume mesh

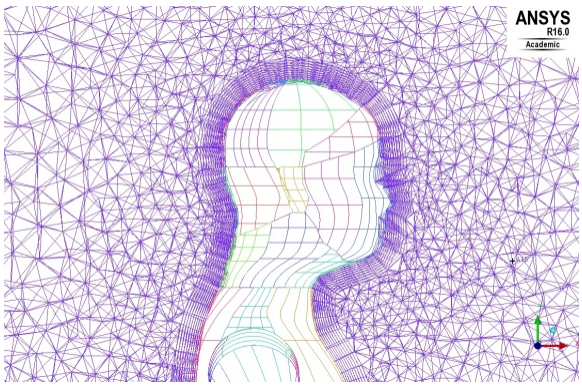

Figure 5 Detailed volume mesh close to Victoria's head

Secondly, ICEM CFD has been used to generate an unstructured mesh. Since the fan was modelled in CFX as a momentum source, at this stage two bodies have been defined, namely the room itself and the fan. The shell mesh parameters have been set to 'all triangle' and 'patch independent'. In order to generate a robust surface mesh, but also a smooth volume mesh, the mesh has been initially generated using the Octree algorithm, then this volume mesh has been deleted and the quality of the surface mesh increased, and later the final volume mesh has been generated using the Delaunay algorithm. In the final mesh, 10 prism layers were also added to accurately model the boundary layer near surfaces. In the final mesh, the maximum mesh size on the manikin parts is 0.02 m, the maximum volume mesh size is 0.128

m, and the initial height of the prism layers is 0.002 m for the manikin and 0.004 m elsewhere. The surface mesh is shown is Figure 3, the volume mesh in Figure 4 and 5.

The final mesh has then been imported into CFX. The boundary conditions for the manikin have always to match the requirements of the IESD-Fiala model, while the other surfaces have been modelled as fixed temperature surfaces. S_{air}, T_{air} and RH at the inlet have been defined according to the measured values. Only T_{air} and RH have been defined at the opening, plus a 2.69 loss coefficient, which is equivalent to a discharge coefficient of 0.61. For the moist air inside the room, the initial mass fraction and buoyancy reference density have been calculated based on the RH and T_{air} initial values.

Similarly to previous studies (Cropper et al, 2010), the SST k-ω turbulence model has been chosen for its accuracy and robustness, and a discrete transfer radiation model has been used to model the long-wave radiation heat exchange between the body and surrounding surfaces. Transient simulations have been performed to better model the real transient heat exchange process. A second order backward Euler scheme, and high resolution advection scheme and turbulence numerics have been used. The double precision option has also been selected.

Convergence criteria have been set equal to 1e-05 for the RMS residuals and 0.01 for the conservation target. Moreover, the RMS Courant number was monitored aiming for values smaller than five. Since it is an implicit code, CFX does not require the Courant number to be small for stability, but this still leads to more accurate results. To reach this target, the chosen time step has been 0.5 s for the case without fan, and 0.2 s for the other. The total time simulated in both cases is 10 minutes.

For the configuration with the active fan, four simulations have been completed, each of which has a different value for the momentum source. Although perfectly matching the actual speed profile is a very complex task, using this approach it has been possible to assess how sensitive the DTS is to small variation of the S_{air}.

Finally, the parameters within the thermal comfort and human regulation model are set. The environmental initial conditions have been matched with those set in CFX, the chosen activity level has been 1.2 met, and the clothing has also been defined in order to represent what Victoria was wearing.

Alongside the main simulations, a mesh sensitivity analysis has been carried out, with the aim of estimating the discretization error and calculating the numerical uncertainty in the fine-grid solution, which is the grid then used for the main simulations. To do so, three increasingly coarse meshes were used (see number of elements N_i in Table 2), a represented dimension h_i to be calculate, and a significant simulated value φ_i has to be used quantify this uncertainty (Celik, 2008). In this research, the T_{air} at 1.1 m above the floor (position of the highest Dantec probe – complete kit) has been chosen since it is close to the manikin and in a central location. The process has been repeated twice and results are reported in Table 2. In the second analysis, a finer mesh was tested.

Table 2

Discretization error calculation (Celik, 2008)

	Analysis 1	**Analysis 2**
N_1	1,297,150	5,685,417
N_2	691,817	1,297,150
N_3	377,870	691,817
h_1	0.03	0.02
h_2	0.04	0.03
h_3	0.05	0.04
r_{21}	1.23	1.64
r_{32}	1.22	1.23
φ_1	25.71	25.70
φ_2	25.72	25.71
φ_3	25.74	25.72
ε_{21}	0.01	0.01
ε_{32}	0.02	0.01
p	0.734787367	1.005076765
φ_{ext}^{21}	25.6	25.7
e_a^{21}	0.000388954	0.000389105
e_{ext}^{21}	0.002342261	0.00060775
GCI_{fine}^{21}	1.76%	0.12%

The mesh chosen for the main simulations is mesh 1 of the first analysis, which has 1297150 elements and a numerical uncertainty equal to 1.76 %. The finest mesh of the second analysis has not been used as the CPU time required to solve it would approximately 10 times higher, but the numerical uncertainty would have been reduced by only 1.64 %.

RESULTS AND DISCUSSION

In this section the results of the simulations are presented and discussed. Firstly, the simulated values are compared with measurements in order to validate the CFD model. Secondly, the computational power required to solve these models is discussed. The last part is then about the relationship between this dynamic thermal comfort model and more traditional ones.

CFD models validation

The key parameters used to validate the models are T_{air} and S_{air}, due to their significant impact on the human thermal sensation and to the fact that they have been measured at several points within the chamber. Although the numerical uncertainty of the CFD simulations has been quantified, 1.76 %, in all images there are error bars only for the measured values, in order to keep the images clearer.

Figure 6 presents the comparison between simulated and measured temperatures for the first

configuration, in which the fan was switched off. Taking into account the uncertainties, there is an excellent agreement at all three measured heights. Moreover, the temperature measured 50 cm above the head is 26.3 °C, and the simulated corresponding value is 26.8 °C, which is within the uncertainty interval. As expected in a buoyancy-driven system, the temperature is stratified and the thermal plume is clearly visible above the head in Figure 7.

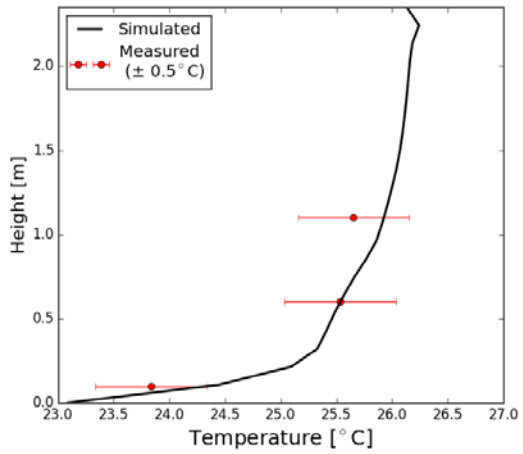

Figure 6 Configuration without fan: simulated and measured air temperatures

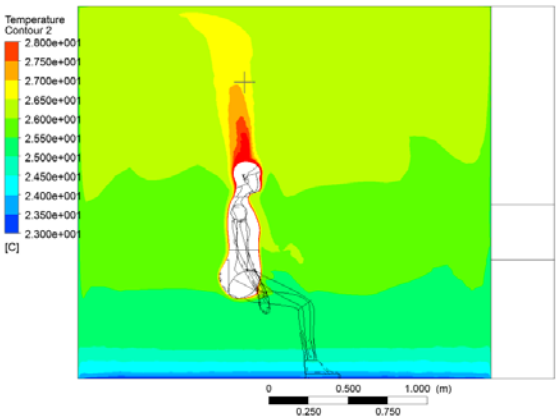

Figure 7 Configuration without fan: air temperature field

In the first configurations, as expected in a mainly buoyancy-driven environment, the S_{air} is low, always below 0.5 m/s. The measured and simulated values within the thermal plume are respectively 0.14 m/s and 0.13 m/s. This agreement supports the choices made while building the model. Previous studies have found slightly higher values, between 0.17 m/s to 0.5 m/s (Yousaf et al. 2011). This difference is likely to be due to the relatively high T_{air} in the chamber in the present study: the difference between the mean density of the air within the room and the value of the warmer air in the plume is smaller, therefore the velocity in the plume is lower.

For the second configuration, in which the fan was operating, achieving a reasonably good agreement between simulated and measured values has been a more challenging task due to the complexity of modelling the effect of the fan. Therefore, the S_{air} at 0.1 m, 0.6 m, and 1.1 m has been taken as the main data source for the validation. As shown in Figure 8, there is one case, namely “simulated 3”, in which simulated values are within the error bars of the measured figures. Although there are only three points of comparison, this seems a good agreement given the small uncertainty in the measurement. In the other three simulations, at one or more heights there are differences that cannot be justified only by the uncertainties, neither in measurement nor in simulations. However, this difference is small, and its effect of the thermal comfort results is discussed later in the paper.

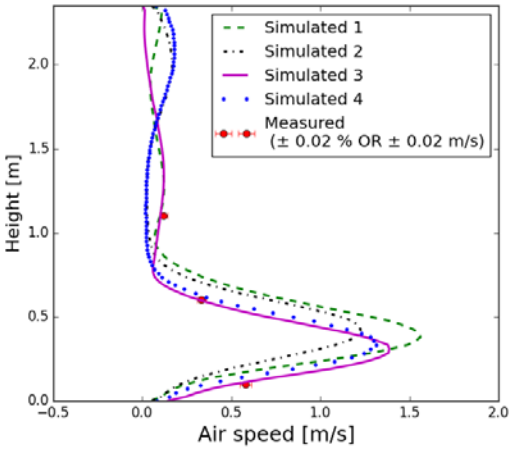

Figure 8 Configuration with fan: simulated and measured air speeds

It is arguable that more comparison points could have been used, but there are at least two reasons to avoid this option. Firstly, these are the three measurements used by the international standards to evaluate the human thermal comfort, therefore this allows for a comparison with traditional models. The second reason is that an elevated number of probes placed within the air stream could affect the stream itself, and therefore the measurement equipment could alter the measured physical quantity. Further work will include more detailed and non-invasive measurement techniques such as particle image velocimetry (PIV).

Due to the action of the fan shown in Figure 9, in this second configuration the air in the room is well mixed and the system is primarily mechanically-driven. As highlighted in Figure 10, simulated and measured T_{air} are in good agreement in each simulation, without any particular difference among the four CFD sets of results. The fact that in both configurations also at the lowest point, 0.1 m, the temperature and velocity match the measured values

suggests that the chosen turbulence model and mesh are appropriate to model this experimental setup.

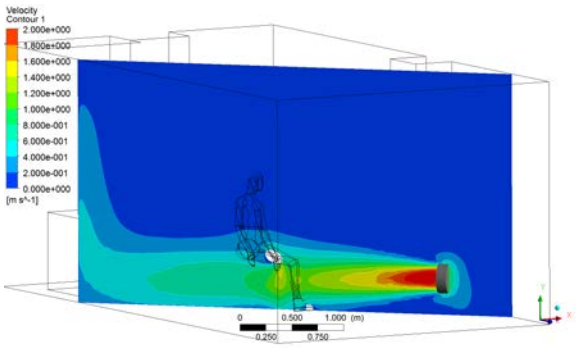

Figure 9 Configuration with fan: air speed field

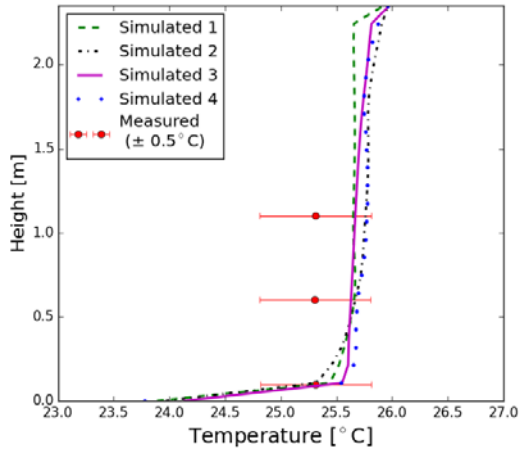

Figure 10 Configuration with fan: simulated and measured air temperatures

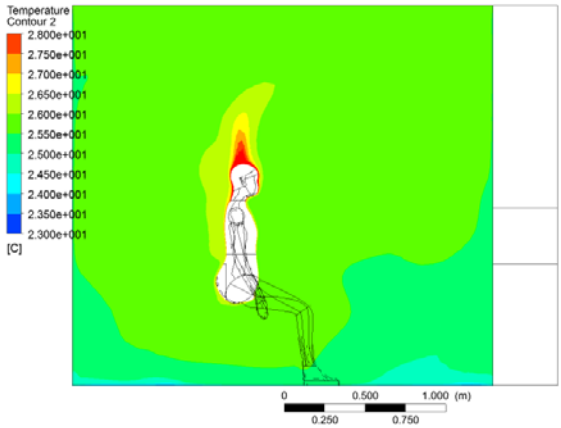

Figure 11 Configuration with fan: air temperature field

Lastly, Figure 11 shows that, due the effect of the fan, the air inside the chamber is well mixed and the thermal plume above Victoria's head is significantly lower than in the configuration without fan (see Figure 7).

Required computational power

Simulations were run on the High Performance Computer System at Loughborough University, a 2460-core 64-bit Intel Xeon cluster. 12 cores were used in these simulations in order to make efficient use of the cluster architecture.

Table 3 Duration of the simulations

Simulation	Total CPU time
Without fan	18 h, 5 m
With fan - 1	1 d, 12 h, 8 m
With fan - 2	1 d, 11 h, 29 m
With fan - 3	1 d, 8 h, 18 m
With fan - 4	1 d, 10 h, 55 m

As reported in Table 3, the duration of the simulation without the fan is almost half of the others. This is due to the use of different time steps, respectively 0.5 s and 0.2 s, but same total time, namely 10 minutes. In the four cases with the fan, the duration is quite similar, and the variations are likely to be due to the different values used for the momentum source which represented the effect of the fan. In general, the greater the total simulation time, the longer the simulation, but there is no clear linear relationship. Unless there is a significant change such as a different fan speed, a convergent solution for a single time step is reached faster after the initial time steps.

In the pre-processing, the meshes have been generated using a work station equipped with an Intel Xeon E5520 CPU and 24 GB of RAM. All the other pre- and post-processing activities have been completed using a laptop with an i5-3320M CPU and 8 GB of RAM. The two coarser meshes could have also been generated with this laptop without exceeding its computational resources.

Relationship with traditional thermal comfort model

The coupled model provides two thermal comfort metrics: DTS and PPD (see Figure 12). The former could be compared with the PMV, while the latter with the PPD included in the international standards.

However, due to the different structure and algorithm of the two approaches, DTS and PMV usually do not have the same value. Firstly, the thermal regulation model included in the coupled system is significantly more complex than the Gagge 2-Node model (Gagge et at, 1971) that has been integrated into the PMV calculation in ASHRAE 55 (ASHRAE, 2013). Secondly, the PMV algorithm uses only a unique value for the clothing and for the four environmental variables. For instance, this means that a subject wearing shorts, T-shirt and sweater, and another one wearing long trousers and T-shirt might have fairly similar clothing values in PMV calculation. If then there is a fan blowing air towards them at the same speed, and all the other four variables are the same, the PMV would be identical for two subjects.

However, the different direction of the air velocity, and the fact that the air hits the subject on body parts with different clothing resistance, may generate a different actual thermal sensation. The coupled model can accommodate this and correctly model the two different situations, while the traditional PMV cannot do so. Lastly, the PMV model assumes steady state conditions, while the coupled model requires only some initial and boundary conditions.

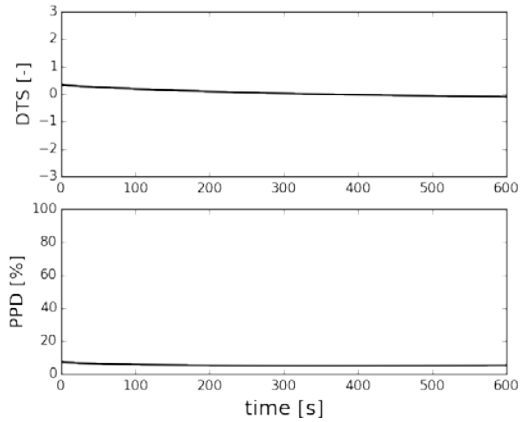

Figure 12 Configuration without fan: DTS and PPD

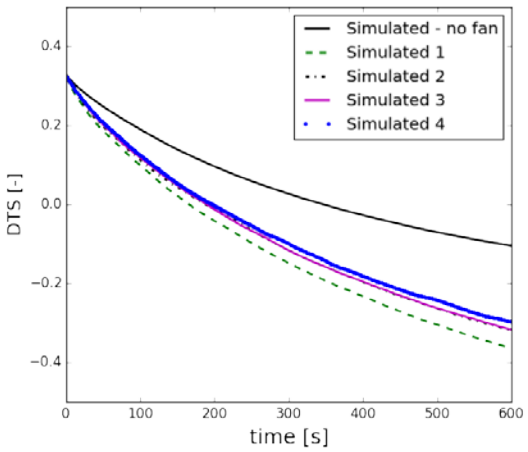

Figure 13 DTS with and without the fan

In figure 13 the DTS results highlight how the fan affects the thermal sensation, but slight variations of the air velocity to not have a significant impact on the DTS. In other words, the DTS does not seem to be that sensitive to a small inaccuracy in the choice of the momentum source. Indeed only in "simulation 3" the simulated and measured S_{air} match (see Figure 8). Further work is needed to understand to which input, or combination of input, the DTS is more sensitive.

CONCLUSIONS

This paper is presenting the initial results of a coupled model made up of two parts: a commercial CFD code, namely ANSYS CFX, and a model of human thermal regulation and comfort, the IESD-Fiala model. In order to validate the simulation results and therefore to fully address the research question, a comparison with experimental data has been completed.

This research suggests that the coupled model is able to predict human thermal comfort in any given indoor configuration, as long as the environment around the human body is accurately modelled. In particular, the DTS is superior to the traditional PMV calculation as both temporal and spatial variation and non-uniform conditions can be taken into account. Therefore, the higher required computational power is compensated by more accurate thermal sensation predictions.

The more the environmental conditions are non-uniform, the longer the time required to calculate the DTS. This is due to the fact that more time is required to accurately replicate these environmental conditions, such as the fan effect, within the CFD model, and also the duration of each simulation is usually longer.

Lastly, comparing simulated and measured values, this paper gives indications about mesh type and resolution, turbulence models, and numerical schemes that can be used to generate a realistic model of the environment around a human body. This is not only applicable to thermal comfort research, but also to any other situation in which CFD is used to study the interaction between people and the surrounding environment.

Limitations and future work

Firstly, a wider range of scenarios is being analysed, chosen from a set of configurations that have been defined based on studies in real buildings, both domestic and commercial, across a wide variety of international locations.

Secondly, a comprehensive sensitivity analysis is needed to identify the effect of each input on the DTS, and therefore to understand the required minimum accuracy of each input. This includes both CFD assumptions, and variables such as the metabolic rate and the clothing resistance.

Thirdly, the IESD-Fiala model was validated by previous studies, but the validation dataset only included studies with adult real human participates from Western countries. Since specific groups such as school children are likely to perceive thermal sensation differently, research is needed to adapt the model to that particular group.

Lastly, on the CFD side, the computational resources required to simulate longer periods and multiple occupants will be assessed. Alongside an increased time required to achieve a converged solution, the coupling process is also likely to become more complex.

ACKNOWLEDGEMENT

This research was financially supported by the Engineering and Physical Sciences Research Council (EPSRC) via the London-Loughborough Centre for Doctoral Research in Energy Demand (LoLo), and by the British Council under the Global Innovation Initiative, the latter involving an international research collaboration between UC Berkeley (USA), CEPT University (India), Loughborough University and De Montfort University (UK). The authors express their gratitude for this support.

REFERENCES

ANSYS. http://www.ansys.com/Products/ Simulation +Technology/FluidDynamics/Fluid+ Dynamics+Products/ANSYS+CFX, last access 25.06.2015

ASHRAE. Standard 55-2013: Thermal Environmental Conditions for Human Occupancy. Atlanta: American Society of Heating, Refrigerating and Air-Conditioning Engineers, Inc.; 2013.

Celik I. Procedure for Estimation and Reporting of Uncertainty Due to Discretization in CFD Applications. ASME. J. Fluids Eng. 2008;130(7):078001-078001-4.

Cook M, Yang T, Cropper P. Thermal comfort in naturally ventilated classrooms: application of coupled simulation models. In: Proceedings of Building Simulation 2011: 12th Conference of International Building Performance Simulation Association. Sydney; 2011. p. 2257-2262.

Cropper P, Yang T, Cook M, Fiala D, Yousaf R. Coupling a model of human thermoregulation with computational fluid dynamics for predicting human - environment interaction. Journal of Building Performance Simulation. 2010 Sep;3(3):233-243.

de Dear R, Brager G. Developing an adaptive model of thermal comfort and preference. ASHRAE Transactions. 1998;104:1-18.

Dynamics Dantec. ComfortSense; www.dantecdynamics.com/comfortsense, last

access 15.06.2015

Fanger, P.O., Thermal Comfort. New York, USA: McGraw-Hill; 1970.

Fiala D, Lomas K, Stohrer M. A computer model of human thermoregulation for a wide range of environmental conditions: the passive system. Journal of Applied Physiology. 1999;87:1957-1972.

Fiala D, Lomas K, Stohrer M. Computer prediction of human thermoregulatory and temperature responses to a wide range of environmental conditions. International Journal of Biometeorology. 2001;45(3):143-159.

Foda E, Almesri I, Awbi HB, Sirén K. Models of human thermoregulation and the prediction of local and overall thermal sensations. Building and Environment. 2011;46(10):2023-2032.

Gagge AP, Stolwijk J, Nishi Y. An Effective Temperature Scale Based on a Simple Model of Human Physiological Regulatiry Response. ASHRAE Transactions. 1971;77:247-262.

Gao N, Niu J. CFD Study of the Thermal Environment around a Human Body: A Review. Indoor and Built Environment. 2005;14(1):5-16.

Huizenga C, Zhang H, Arens E. A model of human physiology and comfort for assessing complex thermal environments. Building and Environment. 2001;36(6):691-699.

MeshLab. http://meshlab.sourceforge.net/, last access 15.02.2016

Onset. HOBO U12 sensors; www.onsetcomp.com/products/data-loggers/u12-013, last access 15.06.2015

Rhino. https://www.rhino3d.com/, last access 15.02.2016

Stolwijk JAJ. Mathematical model of thermoregulation. physiological and behavioural temperature regulation. Springfield, IL: Charles C Thomas; 1970.

Yousaf R, Wood D Cook M, Yang T, Hodder S, Loveday D, Passmore M. CFD and PIV based investigation of indoor air flows dominated by buoyancy effects generated by human occupancy and equipment. In: Proceedings of Building Simulation 2011: 12th Conference of International Building Performance Simulation Association. Sydney; 2011. p 1465-1472

Zhai Y, Zhang Y, Zhang H, Pasut W, Arens E, Meng Q. Human comfort and perceived air quality in warm and humid environments with ceiling fans. Building and Environment. 2015;90:178-185